D614G Spike Mutation Increases SARS CoV-2 Susceptibility to Neutralization

Drew Weissman[1]*, Mohamad-Gabriel Alameh[1], Celia C. LaBranche[2], Robert J Edwards[3, 4], Laura Sutherland[3], Sampa Santra[5], Katayoun Mansouri[3], Sophie Gobeil[3], Charlene McDanal[2], Norbert Pardi[1], Pamela A. Shaw[6], Mark G. Lewis[7], Carsten Boesler[8], Uğur Şahin[8], Priyamvada Acharya[3], Barton F. Haynes[3], Bette Korber[9], David C. Montefiori[2]*

[1]Division of Infectious Diseases, University of Pennsylvania Perelman School of Medicine, Philadelphia, PA USA, [2]Duke Human Vaccine Institute & Department of Surgery, Durham, North Carolina USA, [3]Duke Human Vaccine Institute, Duke University School of Medicine, Durham, NC USA, [4]Duke University, Department of Medicine, Durham NC USA, [5]Center for Virology and Vaccine Research, Beth Israel Deaconess Medical Center, Harvard Medical School, Boston, Massachusetts USA, [6]Department of Biostatistics, Epidemiology and Informatics University of Pennsylvania Perelman School of Medicine, Philadelphia, PA USA, [7]Bioqual Inc., Rockville, MD USA, [8]BioNTech, Mainz, Germany [9]T6: Theoretical Biology and Biophysics, Los Alamos National Laboratory, Los Alamos, NM USA.

* Address correspondence to Drew Weissman, drew@pennmedicine.upenn.edu or David Montefiori, david.montefiori@duke.edu.

Abstract

The SARS-CoV-2 Spike protein acquired a D614G mutation early in the COVID-19 pandemic that appears to confer on the virus greater infectivity and now globally is the dominant form of the virus. Certain of the current vaccines entering phase 3 trials are based on the early D614 form of Spike with the goal of eliciting protective neutralizing antibodies. To determine whether D614G mediates neutralization-escape that could compromise vaccine efficacy, sera from Spike-immunized mice, nonhuman primates and humans were evaluated for neutralization of pseudoviruses bearing either D614 or G614 Spike on their surface. In all cases, G614 Spike pseudovirions were moderately more susceptible to neutralization, indicating this is not an escape mutation that would impede current vaccines. Rather, the gain in infectivity provided by D614G came at the cost of making the virus more vulnerable to neutralizing antibodies.

There is an urgent worldwide need to develop a safe and effective vaccine to help end the COVID-19 pandemic. SARS-CoV-2, the etiologic agent of COVID-19, is a novel coronavirus that was first reported in Wuhan, China in December, 2019 and four months later was declared a pandemic by the World Health Organization. Vaccine efforts began shortly after the first sequence of the virus was made available in January 2020[1]. Presently, at least 23 SARS-CoV-2 vaccines are in clinical trials (https://www.who.int/publications/m/item/draft-landscape-of-covid-19-candidate-vaccines). Because of the urgency and time required to develop a vaccine, most COVID-19 vaccines entering phase 3 trials are based on an early index strain of the virus. These vaccines focus on the viral Spike protein with the goal of eliciting protective neutralizing antibodies.

The trimeric Spike protein mediates virus attachment and entry into host cells[2]. Each monomer is comprised of an S1 subunit, which contains the receptor binding domain (RBD), and an S2 subunit that mediates membrane fusion[3]. The RBD is the primary target of neutralizing antibodies, though the N-terminal domain and other regions of Spike are also known to possess neutralization epitopes[2,4-11]

Early in the pandemic, the virus acquired a mutation, D614G, in the Spike protein that rapidly increased in frequency and is now the dominant form of the virus globally[12]. The pattern of spread, combined with increased infectivity in vitro, suggests the mutation gave the virus a fitness advantage for transmission[12,13]. The mutation is also associated with higher virus loads in respiratory secretions but does not appear to increase virulence[12]. A critical question is whether this mutation also mediates neutralization-escape that may reduce the effectiveness of vaccines in general and especially ones based on the D614 version of the Spike immunogen.

Here, we addressed this question using sera from Spike-immunized mice, nonhuman primates and humans. Neutralization was measured in 293T/ACE2 cells using lentivirus particles pseudotyped with full-length SARS-CoV-2 Spike containing either D614 or G614. As this was the only difference between the pseudoviruses, any change in phenotype can be directly attributed to D614G. Assays were performed with nearly equivalent amounts of input virus doses (relative light unit (RLU) in virus control wells were 501-840x background in all assays).

Mice, rhesus macaques, and humans were immunized with the nucleoside-modified mRNA-LNP vaccine platform[14,15] and one of four different forms of the Spike immunogen, including monomeric and trimeric secreted RBD and diProline stabilized[3,16,17] or Wuhan index strain[1] with a mutated furin cleavage site cell associated trimeric Spike. The furin mutant potentially stabilizes the full-length Spike and maintains the association of the S1 and S2 subunits[16]. Pseudoviral neutralization titers were calculated as 50% and 80% inhibitory doses (ID_{50} and ID_{80}, respectively).

A total of forty mice were immunized twice at a 4-week interval with nucleoside-modified mRNA encoding the diProline stabilized cell surface D614 Spike[3,16,17] in four

equal sized groups, with varying dose and route of vaccine administration. This is the immunogen being employed in the Moderna vaccine entering phase 3 clinical trials (mRNA-1273)[18]. Immunizations were performed by the intradermal (ID) and intramuscular (IM) routes with 10 and 30 μg doses. Preimmune and serum 4 weeks after the second immunization were analyzed for neutralization of pseudoviruses with the D614 and G614 sequences. Preimmune sera from all mice scored negative. At 4 weeks after the second immunization, a relative increase in NAb titer for G614 over D614 was observed for each animal (Figures 1a and S1a, Table S1); analyses were done both as a single group and separately by dose and route. Across all routes and doses (N=40), the geometric mean for the G614:D614 ratio was 5.16-fold ($p < 0.001$) for ID_{50} and for 4.44 for ID_{80} ($p<0.001$). Similar patterns were seen across the 10 μg and 30 μg doses and for both IM and ID routes (Table 1). Table 1 shows the geometric mean for the ratio of G614:D614 NAb titers across route and doses, which ranged from, 3.87 to 6.49 ID_{50} and 4.29-4.57 ID_{80} with $p<0.001$ for all comparisons.

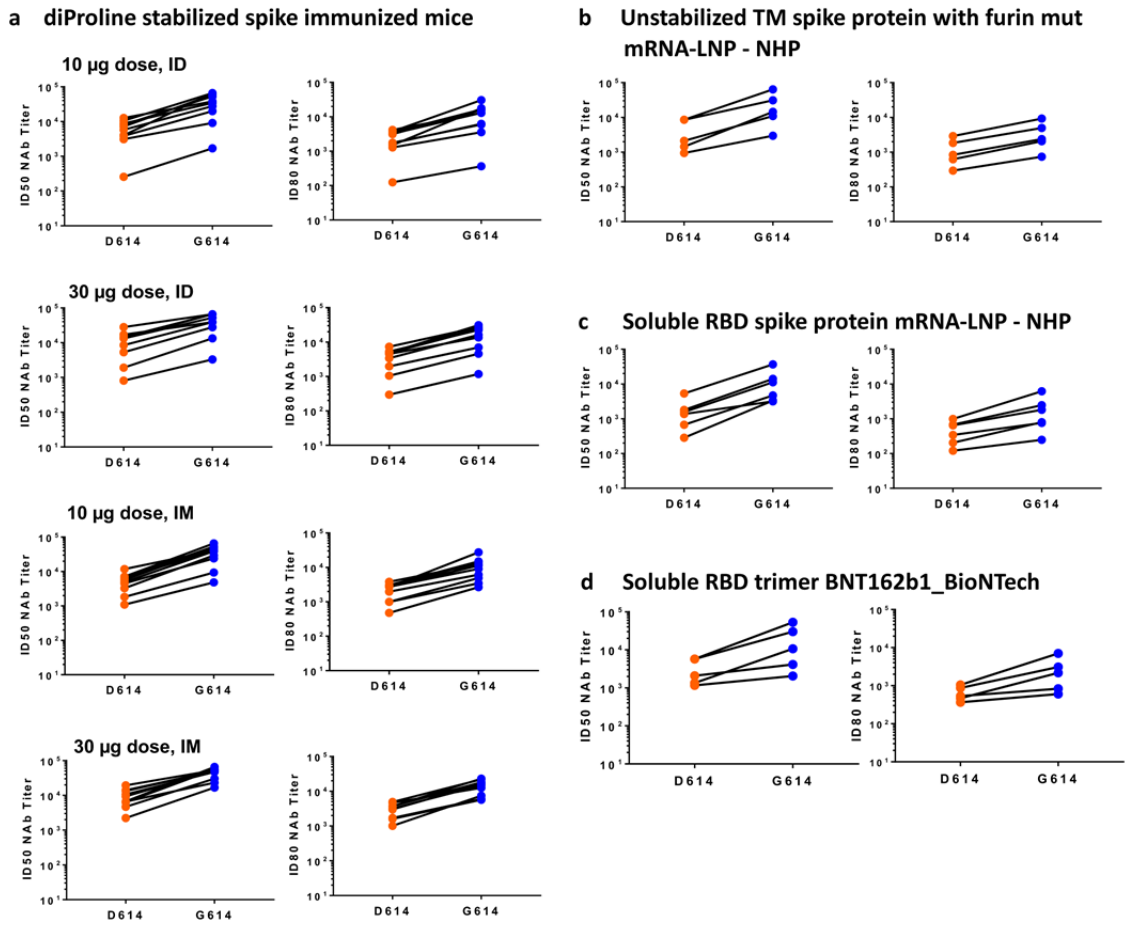

Figure 1. The G614 Spike is neutralized at a higher level than the D614 Spike by sera from mice, rhesus macaques, and humans immunized with nucleoside-modified mRNA-LNPs encoding RBD and full-length Spike immunogens. **(a)** Sera from mice (10 animals/group) immunized twice at a 4-week interval with nucleoside-modified mRNA-LNPs encoding the Wuhan sequence of Spike (D614) with diProline stabilization mutations obtained 4 weeks after the second immunization were tested for neutralization against pseudoviruses with the D614

and G614 variants of Spike. Sera from macaques immunized twice at a 4-week interval with nucleoside-modified mRNA-LNPs encoding the Wuhan sequence of Spike (D614) with a mutated furin cleavage site (n= 5) **(b)** or secreted RBD monomers (n= 6) **(c)** obtained 4 weeks after the second immunization were tested for neutralization against pseudoviruses with the D614 and G614 variants of Spike. **(d)** sera from 5 humans immunized twice at a 3-week interval with nucleoside-modified mRNA-LNPs encoding a secreted RBD trimer. Each dot represents one mouse, macaque, or human. The line connects analyses from individual animals or humans.

	Intramuscular		Intradermal	
Dose	ID_{50}	ID_{80}	ID_{50}	ID_{80}
10 µg	6.49 (p<0.001)	4.50 (p<0.001)	5.60 (p<0.001)	4.41 (p<0.001)
30 µg	5.16 (p<0.001)	4.57 (p<0.001)	3.87 (p<0.001)	4.29 (p<0.001)

Table 1: Geometric mean (ratio t-test p-value) for the ratio of G614:D614 neutralizing antibodies measured in murine sera 4 weeks post second immunization with 10 or 30 µg of diProline stabilized Wuhan sequence Spike encoding mRNA-LNPs, administered via either IM or ID route, with 10 mice per group.

Eleven rhesus macaques were immunized with the nucleoside-modified mRNA-LNP vaccine platform using 2 different immunogens by the IM route (50 µg). The first encoded the Wuhan index strain sequence[1] cell surface Spike protein with a mutated furin cleavage site (furin mut). The second encoded the RBD domain as a secreted monomer. Sera obtained at baseline and 4 weeks after the second immunization were assessed for neutralization of the D614 and G614 variants (Figure 1b and c, Figure S1b and c, Table S1). Baseline (pre-immune) sera were all negative. Post-immunization sera exhibiting greater neutralization of the G614 variant virus for both immunogens. For the cell surface Spike immunogen with a mutated furin site (N=5), the geometric mean for the G614: D614 ID_{50} NAb titer ratio was 5.37-fold ($p = 0.001$) and for ID_{80} was 2.89-fold ($p < 0.001$) (Figure 1b). For the soluble RBD (N=6), the G614:D614 ID_{50} NAb titer ratio had a geometric mean of 6.45-fold ($p < 0.001$) and for ID_{80} was 3.22-fold ($p< 0.001$) (Figure 1c). The observation that the G variant was more sensitive to antibodies induced by both a D614 containing cell surface Spike trimer and an RBD secreted monomer suggests that the G614 mutation increases RBD mediated neutralization.

Preliminary results from a phase 1/2 clinical trial using the nucleoside-modified mRNA-LNP vaccine platform that delivered a secreted RBD trimer was recently published and demonstrated potent ELISA binding and neutralization in all subjects at all tested doses, 10, 30, and 100 µg[19]. Virus neutralizing titers after the second immunization of 10 and 30 µg were 1.8-fold and 2.8-fold greater, respectively, than a convalescent serum panel from SARS-CoV-2 infected patients[19], although the convalescent patients had a wide range and were older than vaccinated subjects.

Sera obtained preimmunization and 7 days after the second immunization with 50 µg (N=3), 30 µg (N=1), and 10 µg (N=1) of human subjects from a phase 1 trial performed in Germany using the same vaccine were analyzed for neutralization of the D614 and G614 Spike variant pseudoviruses. Similar to the data in murine and NHP

immunizations, the G614 pseudovirus was more potently neutralized compared to the D614 pseudovirus by the same serum samples (Figures 1d and S1d, Table S1). The geometric mean of the G614:D614 ID_{50} NAb titer ratio was 4.22-fold (p = 0.014) and for ID_{80} was 3.1-fold (p = 0.017). No neutralizing activity was detected in the corresponding preimmune sera.

The observation that sera from macaques and humans immunized with RBD-only immunogens also enhanced neutralization of the G614 pseudovirus suggested that the elicited response was RBD-directed, and the neutralization enhancement was due to a structural change in the expressed Spike. To evaluate this possibility, we used negative stain electron microscopy (EM) and single particle reconstruction coupled with 3D classification to determine the structure and variability of the two variants in furin-deficient Spike ectodomain (Figure S2) constructs. The D614 variant showed two classes (Figure 2A), called “3-down” or “1-up” in reference to their RBD positions. The D614 variant showed a roughly equal proportion of the 3-down to 1-up states (54% versus 46%) (see methods), consistent with the findings observed by cryo-EM[20]. The G614 variant also showed 3-down and 1-up structures (Figure 2B); however, the 1-up state was more heavily populated, 82%, in the G614 variant. This shift to the 1-up state as the dominant form in the Spike ectodomain demonstrates an allosteric effect of the D614G mutation on the RBD conformation, and suggests a mechanism for the enhanced neutralization susceptibility of the G614 variant.

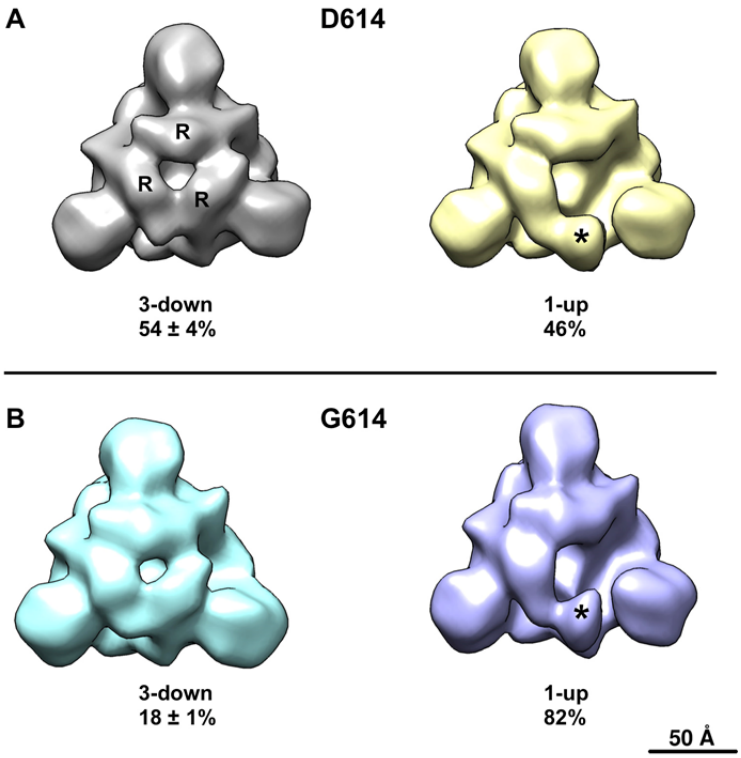

Figure 2. Negative stain electron microscopy reconstructions of expressed Spike constructs following 3D classification. View is looking down the 4-fold trimer axis onto the S1 domain. (A)

D614 variant showing the 3-RBD-down structure on the left with individual RBDs labeled (R), and the 1-RBD-up structure on the right with the up RBD labeled (asterisk). Fraction of particle images that sorted into each class indicated below, expressed as average ± standard deviation, N=3 each. (B) G614 variant also showing 3-down and 1-up structures.

Soon after the G614 mutation in Spike appeared early in the pandemic it rapidly replaced the D614 variant in many countries[12]. This mutation is associated with increased infectivity[12,13] when tested in in vitro model systems. Over 100 vaccines using various platforms and immunogens are being developed to combat COVID-19 and end the devastating financial, societal, and health burdens. Currently, 23 vaccines are in clinical testing, some of which will soon enter phase 3 trials. Most SARS-CoV-2 vaccines were originally designed using the D614 variant of the Spike protein, which was present in the first sequence of SARS-CoV-2 from Wuhan[1]. The most critical finding that will ease the concern for most current vaccines in clinical trials is the finding that the SARS-CoV-2 Spike protein with the G614 mutation is neutralized at a higher level by serum from vaccinated mice, NHPs, and humans that used immunogens derived from the D614 variant of the virus.

D614 is on the surface of the Spike protomer. It can potentially form contacts with a neighboring trimer subunit. The recently published cryo-EM structure of the SARS-CoV-2 Spike demonstrates that the D614 sidechain can form a hydrogen bond with the neighboring protomer T859[3]. This interaction may be critical, as it may bridge residues from the S1 region of one protomer to the S2 region of an adjacent protomer. This interaction would bracket the furin and S2 cleavage sites. Potentially, it could reduce shedding of S1 from viral-membrane-bound S2 and the introduction of G614 would increase S1 release. Our structural data demonstrates that, in the context of the stabilized ectodomain, this mutation leads to an increase in the percent of 1 RBD region per trimer being in the up position, which is necessary for binding to ACE2 and infection of target cells (Figure 2). A recent publication demonstrated a similar effect of the G614 mutation to increase the number of RBDs in the up position[21]. Using an alternative structural analysis method, extensive microsecond timescale atomistic molecular dynamics simulations, reveal that in the G-form, the inter-protomer interactions in the Spike trimer become more symmetric compared to the D-form. This equalization of inter-protomer energetics results in a higher population of one-up Spike conformations, leading to increased encounter between RBD and ACE2 receptor and greater exposure of RBD domain for neutralization (Gnana, personal communication to be replaced with Biorxiv).

Potential drawbacks to our studies include: 1) while we studied 4 different variations of the Spike immunogen, we only used a single type of vaccine, the nucleoside-modified mRNA-LNP platform (reviewed in [15,22]). This platform is recognized as an outstanding new approach that will enter phase 3 clinical trials by 2 separate pharmaceutical/biotech companies, Moderna and Pfizer/BioNTech. The results of phase 1 clinical trials by Pfizer/BioNTech and Moderna demonstrated that all immunized subjects safely developed neutralizing responses[18,19]. 2) We performed pseudovirus neutralization assays. While these assays are considered excellent methods to measure neutralization and are used for the development of many viral vaccines, live

virus neutralization or animal challenges would offer additional methods to measure vaccine response to the G614 variant. As with the pseudovirus assay, assays with live SARS-CoV-2 are performed with viruses that are produced and assayed in cell lines; neutralization assays that use natural target cells of the respiratory system are technically challenging, low throughput and difficult to standardize. 3) Our structural studies were performed in the context of a furin cleavage-deficient Spike ectodomain. While this soluble ectodomain has been shown to be a good mimic of the native Spike, and the shift in the proportion of RBD “up” conformation between the D614 and G614 forms suggest an allosteric effect of the D614G mutation on the RBD conformations, the structures of the native Spike may have some differences from what we observe in the context of the ectodomain.

We demonstrate that vaccinated mice, NHPs, and humans using the nucleoside-modified mRNA-LNP vaccine platform encoding 4 different SARS-CoV-2 Spike immunogens generate antibody responses that not only recognize the G614 mutation that has taken over the pandemic in many countries and has demonstrated increased infectivity[13 12], they have stronger titers of neutralization to this virus variant. The mechanism appears to be that the mutation increases the up formation of the RBD in the Spike trimer, increasing the exposure of neutralization epitopes. Twenty-three vaccines are currently in clinical trial testing. Most of the immunogens used were either derived from the initial D614 virus or contain this mutation in the Spike. The observation that the G614 variant that has replaced the original D614 mutation in the SARS-CoV-2 Spike throughout much of the world is not an escape mutation and, in fact, is better neutralized by sera from mice, NHPs, and humans immunized with immunogens containing or derived from the D614 viral Spike alleviates a major concern in the development of an effective SARS CoV-2 vaccine.

Methods

Ethics statement

All in vivo experiments described in this manuscript were randomized double-blinded and approved by the University of Pennsylvania (UPenn) IACUC. All protocols, experimentation and animal manipulation adhered to the Guide for the Care and Use of Laboratory Animals by the Committee on Care of Laboratory Animal Resources Commission on Life Sciences, National Research Council.

mRNA production

N^1-methylpseudouridine modified mRNA was produced as previously described [23] using T7 RNA polymerase (MegaScript, ThermoFisher Scientific, Waltham, MA, USA) on Not-I/AlfII double digested and linearized plasmids encoding codon-optimized di-proline modified pre-fusion SARS-CoV-2 Spike (Wuhan Hu-1 complete genome, GenBank: MN908947.3), full length S-fm protein (RRAR furin cleavage site abolished), and RBD. In vitro transcribed (IVT) mRNAs were co-transcriptionally capped using the CleanCap system (TriLink Biotechnologies, San Diego, CA, USA), and purified using a cellulose-based chromatography method [24]. All IVT mRNAs were analyzed on agarose (1.4 % w/v, 1X TAE buffer) for integrity, and subjected to additional quality control to rule out double stranded RNA (dsRNA) contamination and endotoxin contamination prior to formulations into lipid nanoparticles (LNPs), as described [25].

Production of mRNA-LNP

Lipid nanoparticles (LNPs) used in this study contain ionizable lipids proprietary to Acuitas /DSPC/Cholesterol/PEG-Lipid [26]. Encoding mRNA was encapsulated in LNPs using a self-assembly process in which an aqueous solution of mRNA at 4.0 pH was rapidly mixed with a solution containing the aforementioned lipids premixed at mol/ mol percent ratio of 50:10:38.5:1.5 and dissolved in ethanol. mRNA was encapsulated into LNPs at a nucleic acid to total lipid ratio of ~0.05 (wt/wt) and aliquoted at a nucleic acid concentration of ~1 mg/ml. All LNPs were characterized post-production at Acuitas pharmaceutical (Vancouver, BC, Canada) for their size, surface charge using a Malvern Zetasizer (Zetasizer Nano DS, Malvern, UK), encapsulation efficiency, and shipped on dry ice and stored at -80°C until use.

Administration of test articles (immunization) and blood collection

8-12 week old Balb/c mice were immunized with either 10 μg of mRNA-LNPs via the intramuscular (IM) route of administration using a 29G X1/2'' Insulin syringe. Mice received a booster injection on day 28 (4 weeks). Blood was collected at day 0, 28 and 56 through the retro-orbital route using non heparinized micro hematocrit capillary tubes (ThermoFisher Scientific,Waltham, MA, USA). Serum was separated by centrifugation (10 000 g, 5 min) using a non-refrigerated Eppendorf 5424 centrifuge (Eppendorf,

Enfield, CT, USA), heat-inactivated (56°C) for 30 minutes, and stored at -20° C until analysis.

Administration of mRNA/LNPs to rhesus macaques

Fifty micrograms of either mRNA/LNPs encoding an unstabilized transmembrane (TM) Spike protein or a monomeric soluble RBD were administered intramuscularly in two sites in the left and right quadriceps on weeks 0, and 4. Monkeys immunized 50 μ g IM; 500 μ L total (250 μ L in R + L quad). Immunizations at wk 0, 4. Animals were anesthetized with ketamine prior to blood draws from the femoral vein. Serum samples were analyzed in 5 macaques immunized with mRNA/LNPs encoding unstabilized TM Spike and in 6 animals immunized with mRNA/LNPs encoding soluble RBD. All studies were performed at Bioqual, Inc, Rockville, MD following IACUC approval.

Clinical trial samples

Serum from subjects enrolled in a phase 1/2 clinical trial of a nucleoside-modified mRNA-LNP vaccine encoding trimeric SARS-CoV-2 RBDs (BNT162b1) were obtained (NCT04380701). Five subjects that received 2 immunizations at a 3-week interval with 10, 30, or 50 μg of mRNA were used. All subjects were considered a single group, as similar serologic data was obtained for each dose and the comparison and calculation of statistical significance was performed within each sample. Serum was obtained prior to the first immunization and 7 days after the second immunization.

SARS-CoV-2 pseudovirus neutralization assay.

SARS-CoV-2 neutralization was assessed with Spike-pseudotyped viruses in 293T/ACE2 cells as a function of reductions in luciferase (Luc) reporter activity. 293T/ACE2 cells were kindly provided by Drs. Mike Farzan and Huihui Mu at Scripps. Cells were maintained in DMEM containing 10% FBS and 3 μg/ml puromycin. An expression plasmid encoding codon-optimized full-length Spike of the Wuhan-1 strain (VRC7480), was provided by Drs. Barney Graham and Kizzmekia Corbett at the Vaccine Research Center, National Institutes of Health (USA). The D614G amino acid change was introduced into VRC7480 by site-directed mutagenesis using the QuikChange Lightning Site-Directed Mutagenesis Kit from Agilent Technologies (Catalog # 210518). The mutation was confirmed by full-length Spike gene sequencing. Pseudovirions were produced in HEK 293T/17 cells (ATCC cat. no. CRL-11268) by transfection using Fugene 6 (Promega Cat#E2692) and a combination of Spike plasmid, lentiviral backbone plasmid (pCMV ΔR8.2) and firefly Luc reporter gene plasmid (pHR' CMV Luc)[27] in a 1:17:17 ratio. Transfections were allowed to proceed for 16-20 hours at 37°C. Medium was removed, monolayers rinsed with growth medium, and 15 ml of fresh growth medium added. Pseudovirus-containing culture medium was collected after an additional 2 days of incubation and was clarified of cells by low-speed centrifugation and 0.45 μm micron filtration and stored in aliquots at -80°C. $TCID_{50}$ assays were performed

on thawed aliquots to determine the infectious dose for neutralization assays (RLU 500-1000x background, background usually averages 50-100 RLU).

For neutralization, a pre-titrated dose of virus was incubated with 8 serial 3-fold or 5-fold dilutions of serum samples in duplicate in a total volume of 150 µl for 1 hr at 37°C in 96-well flat-bottom poly-L-lysine-coated culture plates (Corning Biocoat). Cells were suspended in TrypLE express enzyme solution (Thermo Fisher Scientific) and immediately added to all wells (10,000 cells in 100 µL of growth medium per well). One set of 8 control wells received cells + virus (virus control) and another set of 8 wells received cells (background control). After 66-72 hrs of incubation, medium was removed by gentle aspiration and 30 µL of Promega 1X lysis buffer was added to all wells. After a 10 minute incubation at room temperature, 100 µL of Bright-Glo luciferase reagent was added to all wells. After 1-2 minutes, 110 µL of the cell lysate was transferred to a black/white plate (Perkin-Elmer). Luminescence was measured using a PerkinElmer Life Sciences, Model Victor2 luminometer. Neutralization titers are the serum dilution at which relative luminescence units (RLU) were reduced by 50% and 80% compared to virus control wells after subtraction of background RLUs. Serum samples were heat-inactivated for 30 minutes at 56°C prior to assay.

Protein expression and purification

SARS-CoV-2 ectodomain constructs[3] were produced and purified as follows. Genes encoding residues 1−1208 of the SARS-CoV-2 S (GenBank: MN908947) with a "GSAS" substitution at the furin cleavage site (residues 682–685), with and without proline substitutions of residue K986 and V987 (S-GSAS/PP or S-GSAS), a C-terminal T4 fibritin trimerization motif, an HRV3C protease cleavage site, a TwinStrepTag and an 8XHisTag were synthesized and cloned into the mammalian expression vector pαH. The S-GSAS template was used to include the D614G mutation (S-GSAS(D614G)). Plasmids were transiently transfected into FreeStyle-293F cells using Turbo293 (SpeedBiosystems). Protein was purified on the sixth day post-transfection from filtered supernatant using StrepTactin resin (IBA), followed by size-exclusion chromatography (SEC) purification using a Superose 6 10/300 GL column (GE healthcare) with equilibrated in 2mM Tris, pH 8.0, 200 mM NaCl, 0.02% sodium azide buffer.

Negative-stain electron microscopy

Samples of S-GSAS and S-GSAS (D614G) ectodomain constructs were diluted to 100 µg/ml with room-temperature buffer containing 20 mM HEPES pH 7.4, 150 mM NaCl, 5% glycerol and 7.5 mM glutaraldehyde, and incubated 5 min; then glutaraldehyde was quenched for 5 min by addition of 1M Tris stock to a final concentration of 75 mM. A 5-µl drop of sample was applied to a glow-discharged, carbon-coated grid for 10-15 s, blotted, stained with 2% uranyl formate, blotted and air-dried. Images were obtained with a Philips EM420 electron microscope at 120 kV, 82,000× magnification, and a 4.02 Å pixel size. The RELION program[28] was used for particle picking, 3D classification, and 3D refinements. The number of particle images

that sorted into each class during the classification provides an estimate of the fraction for each state.

Statistical methods

For a given experiment, neutralizing antibody titers for G614 and D614 were measured from serum on each animal and compared using a paired t-test of the logarithm of the antibody titers (ratio t-test). This formally tests whether the ratio of the titer is different from 1. All statistical tests were performed at the 0.05 level in the R software (v3.6.1)[29].

Supplementary tables

Table S1. ID50, ID80 and maximum percent inhibition (MPI) values for all serum samples assayed from mice, nonhuman primates and a phase 1/2 clinical trial.

Supplementary figures

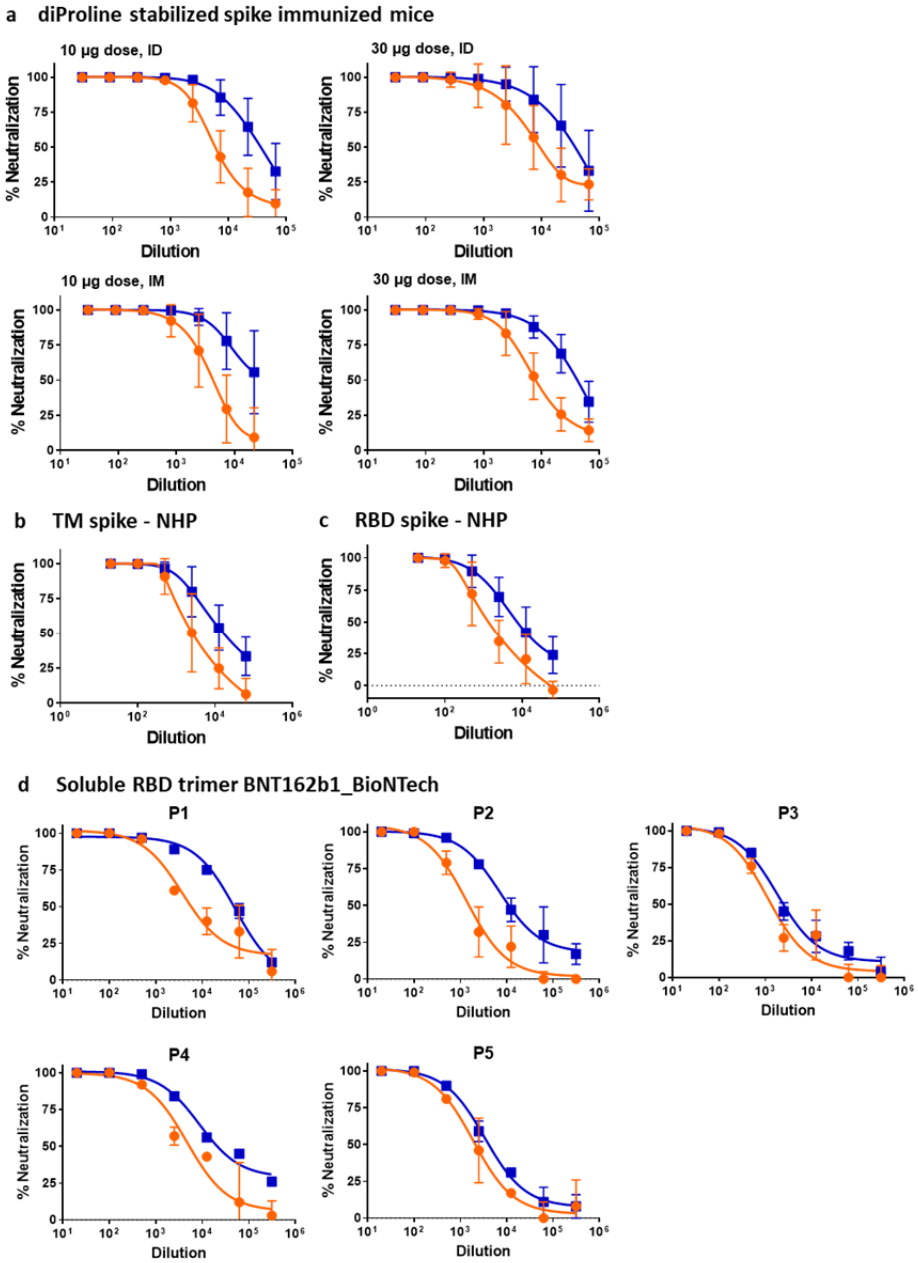

Figure S1. The G614 Spike is more vulnerable to neutralization than D614 Spike by vaccine-elicited serum antibodies. This figure accompanies Figure 1 and its legend. **(a, b and c)** Percent neutralization values at each serum dilution for all animals in each group were averaged. **(d)** Individual neutralization curves for the 5 vaccine recipients in a phase 1/2 clinical trial of nucleoside-modified mRNA-LNPs encoding a secreted RBD trimer. Orange, pseudovuirus bearing D614 Spike; Blue, pseudovirus bearing G614 Spike.

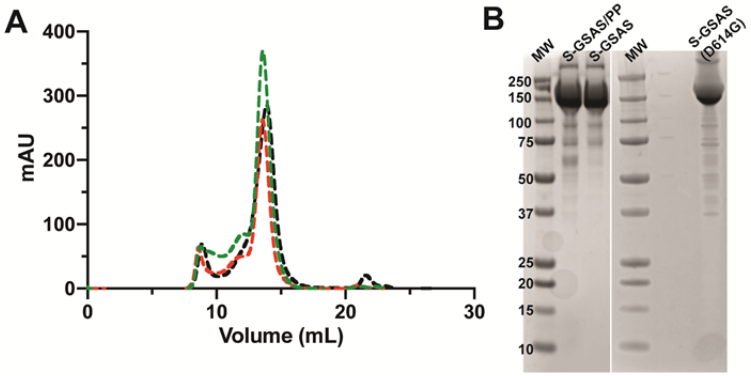

Figure S2. Purification the SARS-CoV-2 S ectodomain. (A) Chromatogram of the size-exclusion purification on a Supersose 6 GL 10/300 column of the Spike ectodomain with proline mutations of residues 986 and 987 and furin cleavage site (residues 682–685) mutated to GSAS (S-GSAS/PP; in black), of the S ectodomain with the proline mutations reverted to the native K and V residues (S-GSAS; in red) and the Spike ectodomain with the mutation D614G (S-GSAS(D614G); in green). **(B)** SDS-PAGE of the purified protein (MW: molecular weight marker; 15 µg/lane).

References

1 Lurie, N., Saville, M., Hatchett, R. & Halton, J. Developing Covid-19 Vaccines at Pandemic Speed. *N Engl J Med* **382**, 1969-1973 (2020), doi:10.1056/NEJMp2005630.

2 Yuan, M. *et al.* A highly conserved cryptic epitope in the receptor binding domains of SARS-CoV-2 and SARS-CoV. *Science* **368**, 630-633 (2020), doi:10.1126/science.abb7269.

3 Wrapp, D. *et al.* Cryo-EM structure of the 2019-nCoV spike in the prefusion conformation. *Science* **367**, 1260-1263 (2020), doi:10.1126/science.abb2507.

4 Brouwer, P. J. M. *et al.* Potent neutralizing antibodies from COVID-19 patients define multiple targets of vulnerability. *Science* (2020), doi:10.1126/science.abc5902.

5 Liu, L. *et al.* Potent Neutralizing Monoclonal Antibodies Directed to Multiple Epitopes on the SARS-CoV-2 Spike. *bioRxiv* (2020), doi:10.1101/2020.06.17.153486.

6 Wec, A. Z. *et al.* Broad neutralization of SARS-related viruses by human monoclonal antibodies. *Science* (2020), doi:10.1126/science.abc7424.

7 Shi, R. *et al.* A human neutralizing antibody targets the receptor-binding site of SARS-CoV-2. *Nature* (2020), doi:10.1038/s41586-020-2381-y.

8 Wu, Y. *et al.* A noncompeting pair of human neutralizing antibodies block COVID-19 virus binding to its receptor ACE2. *Science* **368**, 1274-1278 (2020), doi:10.1126/science.abc2241.

9 Pinto, D. *et al.* Cross-neutralization of SARS-CoV-2 by a human monoclonal SARS-CoV antibody. *Nature* **583**, 290-295 (2020), doi:10.1038/s41586-020-2349-y.

10 Ju, B. *et al.* Human neutralizing antibodies elicited by SARS-CoV-2 infection. *Nature* (2020), doi:10.1038/s41586-020-2380-z.

11 Chi, X. *et al.* A neutralizing human antibody binds to the N-terminal domain of the Spike protein of SARS-CoV-2. *Science* (2020), doi:10.1126/science.abc6952.

12 Korber, B. *et al.* Spike mutation pipeline reveals the emergence of a more transmissible form of SARS-CoV-2. *Biorxiv* **04.29.069054** (2020), doi.

13 Zhang, L. *et al.* The D614G mutation in the SARS-CoV-2 spike protein reduces S1 shedding and increases infectivity. *bioRxiv* (2020), doi:10.1101/2020.06.12.148726.

14 Pardi, N. *et al.* Nucleoside-modified mRNA vaccines induce potent T follicular helper and germinal center B cell responses. *J Exp Med* **215**, 1571-1588 (2018), doi:10.1084/jem.20171450.

15 Alameh, M. G., Weissman, D. & Pardi, N. Messenger RNA-Based Vaccines Against Infectious Diseases. *Curr Top Microbiol Immunol* (2020), doi:10.1007/82_2020_202.

16 Kirchdoerfer, R. N. *et al.* Pre-fusion structure of a human coronavirus spike protein. *Nature* **531**, 118-121 (2016), doi:10.1038/nature17200.

17 Kirchdoerfer, R. N. *et al.* Stabilized coronavirus spikes are resistant to conformational changes induced by receptor recognition or proteolysis. *Sci Rep* **8**, 15701 (2018), doi:10.1038/s41598-018-34171-7.

18 Jackson, L. A. *et al.* An mRNA Vaccine against SARS-CoV-2 - Preliminary Report. *N Engl J Med* (2020), doi:10.1056/NEJMoa2022483.

19 Sahin, U., Muik, A., Derhovanessian, E., Vogler, I., Kranz, L.M., Vormehr, M., Baum, A., Pascal, K., Quandt, J., Maurus, D., Brachtendorf, S., Lörks, V., Sikorski, J., Hilker, R., Becker, D., Eller, A-K., Grützner, J., Boesler, C., Rosenbaum, C., Kühnle, M-C., Luxemburger, U., Kemmer-Brück, A., Langer, D., Bexon, M., Bolte, S., Karikó, K.,

Palanche, T., Fischer, B., Schultz, A., Shi, P-Y., Fontes-Garfias, C., Perez, J-L., Swanson, K-A., Loschko, J., Scully, I-L., Cutler, M., Kalina, W., Kyratsous, C.A., Cooper, D., Dormitzer, P.R., Jansen, K.U., Türeci, O. Concurrent human antibody and T_H1 type T cell responses elicited by a COVID-19 RNA vaccine. *medRxiv* (2020), doi: 10.1101/2020.07.17.20140533.

20 Walls, A. C. *et al.* Structure, Function, and Antigenicity of the SARS-CoV-2 Spike Glycoprotein. *Cell* **181**, 281-292 e286 (2020), doi:10.1016/j.cell.2020.02.058.

21 Yurkovetskiy, L. *et al.* Structural and Functional Analysis of the D614G SARS-CoV-2 Spike Protein Variant. *bioRxiv* **July 16, 2020** (2020), doi.

22 Pardi, N., Hogan, M. J., Porter, F. W. & Weissman, D. mRNA vaccines - a new era in vaccinology. *Nat Rev Drug Discov* **17**, 261-279 (2018), doi:10.1038/nrd.2017.243.

23 Freyn, A. W. *et al.* A Multi-Targeting, Nucleoside-Modified mRNA Influenza Virus Vaccine Provides Broad Protection in Mice. *Mol Ther* **28**, 1569-1584 (2020), doi:10.1016/j.ymthe.2020.04.018.

24 Baiersdorfer, M. *et al.* A Facile Method for the Removal of dsRNA Contaminant from In Vitro-Transcribed mRNA. *Mol Ther Nucleic Acids* **15**, 26-35 (2019), doi:10.1016/j.omtn.2019.02.018.

25 Pardi, N. *et al.* Expression kinetics of nucleoside-modified mRNA delivered in lipid nanoparticles to mice by various routes. *J Control Release* **217**, 345-351 (2015), doi:10.1016/j.jconrel.2015.08.007.

26 Lin, P. J. *et al.* Influence of cationic lipid composition on uptake and intracellular processing of lipid nanoparticle formulations of siRNA. *Nanomedicine* **9**, 233-246 (2013), doi:10.1016/j.nano.2012.05.019.

27 Naldini, L. *et al.* In vivo gene delivery and stable transduction of nondividing cells by a lentiviral vector. *Science* **272**, 263-267 (1996), doi:10.1126/science.272.5259.263.

28 Scheres, S. H. Processing of Structurally Heterogeneous Cryo-EM Data in RELION. *Methods Enzymol* **579**, 125-157 (2016), doi:10.1016/bs.mie.2016.04.012.

29 R. C Team. *A language and environment for statistical computing.* . (2019).